Large-Scale Measurement Layout Optimization Method Based on Laser Multilateration

Ying Sheng [1,2]**, Yukun Wang** [1,2]**, Siwei Liu** [3]**, Cuiping Wang** [3] **and Juntong Xi** [1,2,4,*]

1. School of Mechanical Engineering, Shanghai Jiao Tong University, Shanghai 200240, China
2. Shanghai Key Laboratory of Advanced Manufacturing Environment, Shanghai 200240, China
3. Shanghai Satellite Equipment Research Institute, Shanghai 200240, China
4. State Key Laboratory of Mechanical System and Vibration, Shanghai 200240, China
* Correspondence: jtxi@sjtu.edu.cn

Abstract: Laser multilateration is a measurement method based on the distance intersection of multiple laser trackers which has been widely used in large-scale measurements. However, the layout of laser trackers has a great impact on the final measurement accuracy. In order to improve the overall measurement accuracy, firstly, a measurement uncertainty model based on laser multilateration is established. Secondly, a fast laser intersection detection constraint algorithm based on a k-DOPS bounding box and an adaptive target ball incident angle constraint detection algorithm are established for large-scale measurement scenes. Finally, the constrained layout optimization of the laser trackers is realized by using an improved cellular genetic algorithm. The results show that the optimized system layout can achieve the full coverage of measurement points and has higher measurement accuracy. Compared with the traditional genetic algorithm, the improved cellular genetic algorithm converges faster and obtains a better position layout.

Keywords: large-scale measurement; laser tracker; multilateration; constrained layout optimization; cellular genetic algorithm

1. Introduction

In the measurement site of aerospace, it is necessary to perform precise measurements of large-scale assemblies [1]. A space mast is a widely used aerospace structure that plays an important role in observation, communication, space science, deep space exploration, and other activities [2,3]. The accuracy and stability of large space masts will directly affect the service performance of large aerospace systems, which puts forward a high requirement for measurement technology in large scenes. In recent years, various types of large-scale measurement equipment have been developed, such as laser trackers [4], iGPS [5], machine vision [6], and wMPS [7]. Compared with other equipment, a laser tracker has a wide measurement range and high measurement accuracy and is widely used in manufacturing sites.

Laser multilateration is a mature measurement method that mainly uses multiple laser tracker stations to determine the coordinates of target points. Compared with the measurement of a single laser tracker, laser multilateration only uses the distance measurement value, which can obtain higher measurement accuracy [8]. However, it is difficult to choose the positions and layout of multi-station laser trackers in large spaces, which requires the study of laser tracker station distribution.

Previous studies have been carried out to determine the layout of laser trackers under different conditions. For the multilateral layout of four laser trackers, Takatsuji et al. [9,10] proposed a layout principle wherein four stations cannot be on the same plane. Wang et al. [11] developed a GPU-accelerated light detection algorithm and realized the constrained layout optimization of multiple laser trackers by mode search, genetic algorithm,

and particle swarm optimization. Aguado et al. [12] studied the influence of the spatial angle between laser trackers, the distance, and the visibility of the target point on the measurement uncertainty of the laser tracker, which reduces the volumetric error of the machine tool. Hu et al. [13] simulated and optimized the layout of the laser tracker based on the proposed calibration method, and the result showed that the tri-rectangular pyramid layout was the best layout and could improve measurement accuracy. Zhang et al. [14] studied the in situ measurement method of a large thin-wall tank's ring seam welding and optimized the layout of laser trackers and ERS points using a genetic algorithm. Ren et al. [15] proposed a grid-based placement optimization based on a genetic algorithm and realized the global optimization through the combination of global and local search, which reduced the requirements of the algorithm in the initial layout. Wang et al. [16] proposed an optimization method using the positional dilution of precision (PDOP) as the evaluation factor and realized the evaluation of the optimal laser tracker station by analyzing the distribution law of PDOP at different positions.

In this paper, we proposed a large-scale measurement layout optimization method based on an improved cellular genetic algorithm. Firstly, the measurement uncertainty of spatial points by laser multilateration is obtained. Then, aiming at the problems of light path occlusion and target ball measurement error, the visibility constraint of the laser tracker and the incident angle constraint of the target ball are established. Finally, based on the above constraints, the improved cellular genetic algorithm is adopted to search for the best station distributions in space. The results show that the proposed method can effectively improve measurement accuracy and optimize layout efficiency.

2. Laser Multilateration Measurement Uncertainty

2.1. Measurement Principle of Laser Multilateration

The principle of laser multilateration is shown in Figure 1. Four or more laser trackers are established in space, and the three-dimensional coordinates of the target point are calculated only by the distance from each station to the target ball [17].
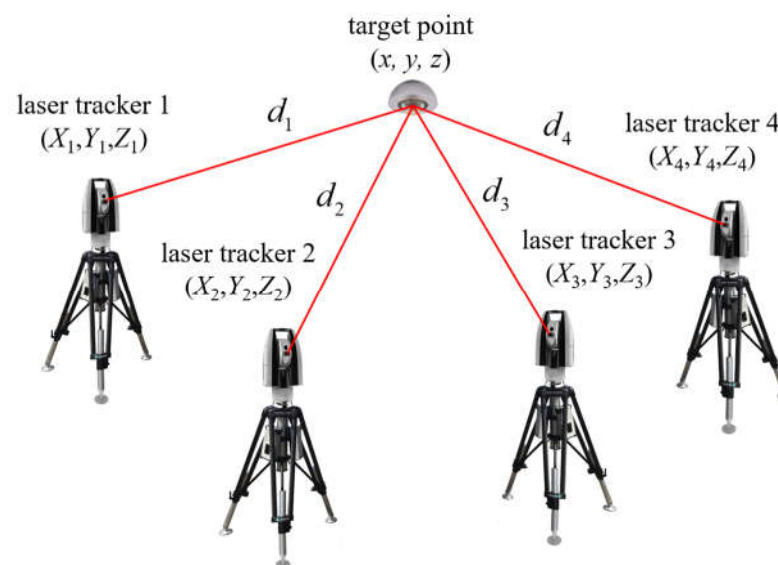

Figure 1. Measurement principle of laser multilateration.

For the four laser tracker stations $(X_j, Y_j, Z_j), j = 1,...,4$, control them to track the same target ball (x, y, z), then the distance d_i from each station to the reflective target ball can be obtained. Tour distance equations can be established as follows.

$$\begin{cases} (X_1 - x)^2 + (Y_1 - y)^2 + (Z_1 - z)^2 = d_1^2 \\ (X_2 - x)^2 + (Y_2 - y)^2 + (Z_2 - z)^2 = d_2^2 \\ (X_3 - x)^2 + (Y_3 - y)^2 + (Z_3 - z)^2 = d_3^2 \\ (X_4 - x)^2 + (Y_4 - y)^2 + (Z_4 - z)^2 = d_4^2 \end{cases} \tag{1}$$

To obtain the coordinate value of the target point, the equations above can be converted into the residual error r_j, which is the difference between the calculated value and the measured value. As shown in formula (2), $\widehat{X_j}, \widehat{Y_j}, \widehat{Z_j}$ are the calculated station coordinates with errors, and $\widehat{d_j}$ is the measured distance value with error. The problem is then transformed into solving the minimum residual sum φ, which can be solved by using the Gauss–Newton method, trust region method, Levenberg–Marquardt method [18], and other methods.

$$r_j = \sqrt{(\widehat{X_j} - x)^2 + (\widehat{Y_j} - y)^2 + (\widehat{Z_j} - z)^2} - \widehat{d_j}, j = 1,...,4 \tag{2}$$

$$\min \ \varphi = \frac{1}{2} \sum_{j=1}^{4} r_j^2 \tag{3}$$

2.2. Spatial Measurement Uncertainty of Target Point

A variety of error factors will be introduced in the measurement process of the laser tracker, which will affect the spatial measurement uncertainty of the target point. For the laser multilateration, the main error sources in the measurement process are the distance measuring error of the laser tracker and the station coordinate error caused by self-calibration. For the spatial point measurement of laser trackers, the input quantity is $I = (d_1, d_2, d_3, d_4, X_1, Y_1, Z_1, ..., X_4, Y_4, Z_4)$, and the unknown quantity is the three-dimensional coordinates of the spatial point $P = (x, y, z)$.

The GUM method is adopted to evaluate the uncertainty of laser multilateration measurement [19]. The input uncertainty is the distance measuring uncertainty of the corresponding laser tracker u_{d_j} and the station coordinate uncertainty $(u_{X_j}, u_{Y_j}, u_{Z_j})$. Since each uncertainty is independent, the final input uncertainty matrix U_1 can be expressed in the form of a diagonal matrix.

$$U_I = diag(u_{d_1}^2, ..., u_{d_4}^2, u_{X_1}^2, u_{Y_1}^2, u_{Z_1}^2, ..., u_{X_4}^2, u_{Y_4}^2, u_{Z_4}^2) \tag{4}$$

The output uncertainty matrix U_P can be obtained by calculating the sensitivity matrix J.

$$U_P = JU_I(J)^T = \frac{dP}{dI}U_I(\frac{dP}{dI})^T \tag{5}$$

Since the laser multilateration is solved by nonlinear optimization, the sensitivity matrix J between the input and output cannot be obtained directly by derivation. When φ reaches its minimum value, its derivative of P is 0, so the sensitivity matrix can be solved by using implicit functions.

$$F(P, I) = \frac{d\varphi}{dP} = 0 \tag{6}$$

$$\frac{dP}{dI} = -\left(\frac{dF(P,I)^T}{dP} \right)^{-1} \frac{dF(P,I)^T}{dI} \tag{7}$$

Finally, the output uncertainty matrix of the target point can be obtained.

$$U_P = \begin{bmatrix} u_x^2 & u_{xy} & u_{xz} \\ u_{yx} & u_y^2 & u_{yz} \\ u_{zx} & u_{zy} & u_z^2 \end{bmatrix} \tag{8}$$

For the target point, its total spatial uncertainty can be expressed as follows.

$$u = \sqrt{u_x^2 + u_y^2 + u_z^2} \tag{9}$$

3. Constraint Conditions for Layout Optimization

3.1. Visibility Constraint

When there is an occlusion between the laser tracker and the reflective target ball, the laser beam will be interrupted, resulting in measurement failure. Therefore, it is necessary to detect the occlusion in the environment and determine whether it will block the laser light path. We simplified the occlusion into a k-DOPs bounding box to achieve the rapid line of sight detection of the laser tracker and return the judgment result of intersection judgment.

In three-dimensional space, a k-DOPs bounding box is a convex polyhedron surrounded by $k/2$ pairs of parallel planes. Each pair of planes is determined by a fixed normal direction $n_j, j = 1,...,k/2$ and can closely surround all mesh vertices of the object. Let the vertex on the object be P_i, as shown in Figure 2.
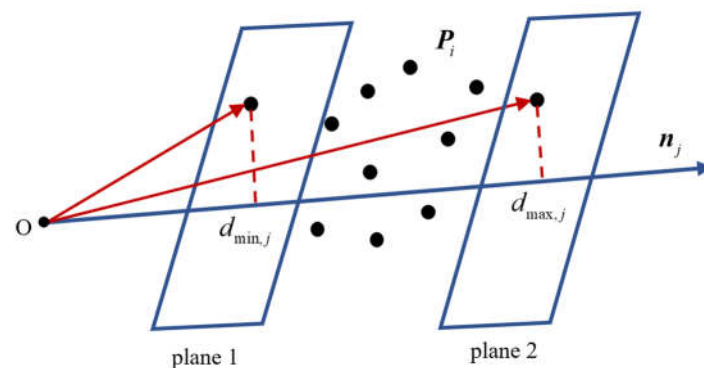

Figure 2. Parallel planes of a k-DOPS bounding box.

Calculate the dot product of any point in the set and the normal direction by formula (10) and take the maximum and minimum values for all results.

$$\begin{cases} d_{max,j} = \max_i \{P_i \cdot n_j\} \\ d_{min,j} = \min_i \{P_i \cdot n_j\} \end{cases} \tag{10}$$

Then, each group of parallel planes can be uniquely determined as the following mathematical expression. For the occlusion in the measurement space, the parameters of the corresponding k-DOPs bounding box can be calculated before layout optimization and can be reused in subsequent intersection judgment to avoid repeated calculations.

$$G_j = \{n_j, d_{max,j}, d_{min,j}\} \tag{11}$$

The projection interval $[t_{min,j}, t_{max,j}]$ of the laser beam from the laser tracker to the reflective target ball on each plane pair is expressed as the following formula.

$$\begin{cases} t_{\min,j=}\dfrac{d_{\min,j}-(S_o\cdot n_j)}{(S_1-S_0)\cdot n_j},\ t_{\max,j=}\dfrac{d_{\max,j}-(S_o\cdot n_j)}{(S_1-S_0)\cdot n_j},\ (S_1-S_0)\cdot n_j>0 \\[4mm] t_{\min,j=}\dfrac{d_{\max,j}-(S_o\cdot n_j)}{(S_1-S_0)\cdot n_j},\ t_{\max,j=}\dfrac{d_{\min,j}-(S_o\cdot n_j)}{(S_1-S_0)\cdot n_j},\ (S_1-S_0)\cdot n_j<0 \end{cases} \tag{12}$$

where S_0 is the selected laser tracker position and S_1 is the target ball position.

The visibility judgment is performed according to formula (13), where $u_{\min}$ is the minimum value among the maximum values of all projection intervals, and $u_{\max}$ is the maximum value among the minimum values of all projection intervals.

$$u_{\min}=\max_j\{t_{\min,j},0\}<u_{\max}=\min_j\{t_{\max,j},1\} \tag{13}$$

When Equation (13) holds, it is considered that the projection interval coincides, which means there is an intersection between the laser beam and the k-DOPs bounding box.

3.2. Incident Angle Constraint

The reflection ball is an important part of laser distance measurement. If the angle of the incident laser beam is too large, the measurement accuracy will be greatly affected. Generally, the target ball is manually rotated to align with the laser emission point, but this process requires repetitive operation and will introduce a large target ball eccentricity error. Therefore, it is necessary to limit the incidence angle of the multiple laser beams so that when multiple stations aim at a reflective target ball simultaneously, they all have a relatively small incidence angle.

For the reflective target ball with the maximum incident angle of $\theta_{\max}$, the incident angle constraint is demonstrated in Figure 3. The incident laser beam needs to be inside the cone with the center of the target ball as the vertex and the apex angle not exceeding $2\theta_{\max}$.
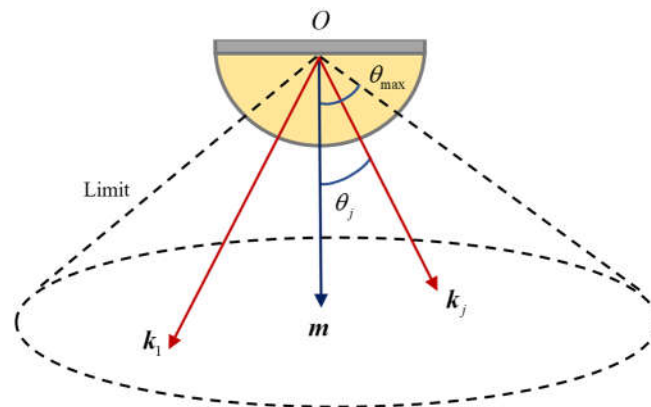

Figure 3. Incidence angle limitation of the target ball.

A separate coordinate system can be established for each target ball, with the center of the target ball as the origin of the coordinate system. The normal direction of the target ball coordinate system is expressed as follows.

$$m=(m_x,m_y,m_z) \tag{14}$$

For all the laser beam vectors, the relative angle between them and the normal vector m needs to be smaller than the maximum angle $\theta_{\max}$. The vector from the selected target

ball center (O_x, O_y, O_z) to the laser tracker station (X_j, Y_j, Z_j) can be expressed as the standard vector, shown in the following formula.

$$k_j = (X_j - O_x, Y_j - O_y, Z_j - O_z) = (k_{x_j}, k_{y_j}, k_{z_j}) \tag{15}$$

$$\sqrt{k_{x_j}^2 + k_{y_j}^2 + k_{z_j}^2} = 1 \tag{16}$$

The cosine of the angle formed by each standard incident vector and the target normal vector is described as follows.

$$\lambda_j = \frac{m_x k_{x_j} + m_y k_{y_j} + m_z k_{z_j}}{\sqrt{m_x^2 + m_y^2 + m_z^2}}, j = 1, ..., N \tag{17}$$

To ensure that the laser incident angle of each station is within the given range, the angle constraints can be transformed into a constrained optimization problem.

$$\min \sum_{j=1}^{N} (1 - \lambda_j)^2, \ \lambda_j \geq \cos\theta_{max} \tag{18}$$

An adaptive weight is introduced based on the above function. For angles close to or larger than θ_{max}, a larger weight is given so that the final optimized incident angle of the multiple stations is relatively small.

$$\min \sum_{j=1}^{N} \frac{1}{1 + \exp(\lambda_j - \frac{1 + \cos\theta_{max}}{2})} \times (1 - \lambda_j)^2, \ \lambda_j \geq \cos\theta_{max} \tag{19}$$

The optimal angle between the normal vector and each incident vector is calculated by using the least-squares method. If the results are all less than θ_{max}, it is considered that the point meets the incident angle constraint, and the simultaneous measurement of the multiple laser trackers can be realized.

4. Layout Optimization Based on an Improved Cellular Genetic Algorithm

The cellular genetic algorithm (CGA) is an evolutionary algorithm that combines a cellular automaton and a genetic algorithm. It enhances the local search ability of the traditional genetic algorithm and ensures a good balance between the global search and local optimization [20].

The process of the CGA is as follows. Each genetic individual is set as a cell, and the genetic population is mapped into a two-dimensional cellular space, as shown in Figure 4. During iteration, each cellular individual is selected, crossed, and mutated with its surrounding neighboring individual to generate new individuals. After that, compare the fitness of the new individual with that of the initial individual. If the fitness is optimized, replace the central individual with the new individual, otherwise, keep the original individual.
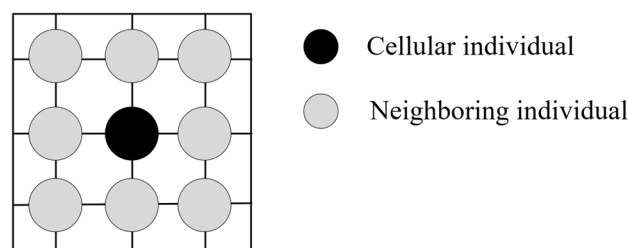

Figure 4. Layout of cellular and neighboring individuals.

In order to ensure the balance between the global search and local optimization of the CGA, the number of times that each cellular individual is not updated in the iterative process is recorded. When the individual has not been updated for a long time, the size of the crossover and mutation operators is adaptively changed, thereby helping the algorithm to jump out of the local optimal solution. For each cellular individual, the corresponding crossover and mutation operators are as follows.

$$P_{c,i} = p_c - \frac{\varepsilon_c}{1 + \exp(\frac{C_i \times m}{M})} \tag{20}$$

$$P_{m,i} = p_m + \frac{\varepsilon_m}{1 + \exp(\frac{C_i \times m}{M})} \tag{21}$$

where p_c and p_m are the initial crossover and mutation operators, respectively; C_i is the number of times that each cell has not been updated; ε_c and ε_m are adjustable constants; m is the current iteration number; and M is the total number of iterations.

Based on the improved CGA, the layout optimization of multiple laser trackers in a large-scale scene is carried out. For the N points that need to be measured in space, the average uncertainty of all points is used as the fitness function of layout optimization.

$$f = \min \frac{\sqrt{u_1^2 + u_2^2 + \cdots + u_N^2}}{N} \tag{22}$$

The layout optimization process based on the improved CGA is shown in Figure 5. First, the position of each laser tracker is encoded and the population is initialized. Second, the visibility constraint and the incident angle constraint are taken as the judgment conditions. If the constraint conditions are not satisfied, the fitness function of the individual is set to an abnormally large value, so that the individual is eliminated in the next iteration loop. Last, the optimal layout that meets the measurement requirements is obtained by genetic operation between the cellular individual and the neighboring individual.
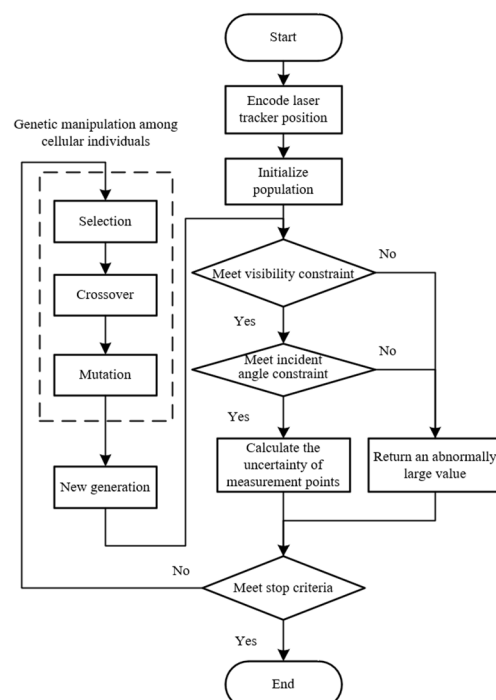

Figure 5. Layout optimization process based on the cellular genetic algorithm.

5. Experiment and Analysis

In order to verify the effectiveness of the above layout optimization algorithm, a simulation experiment was carried out to compare the measurement uncertainty of target points before and after layout optimization in large-scale measurement areas. In order to measure the large space mast in the aerospace manufacturing site, 21 target points are set up in the measurement area, as shown in Figure 6. Set the overall space to $10m \times 20m \times 5m$ and arrange a measurement area of $5m \times 12m$ in the middle, with a height not higher than $2m$. Arrange a rectangular block as the occlusion in the measurement area, and its overall size is $1m \times 1m \times 0.2m$. In order to improve the efficiency of the layout optimization, the entire measurement space is divided into discrete grids, and each grid point corresponds to a feasible position of the laser tracker. Considering the actual cost, a total of four laser trackers are used to measure the target points. The maximum incident angle of the reflective target ball at each measurement point is $\pm 60°$.
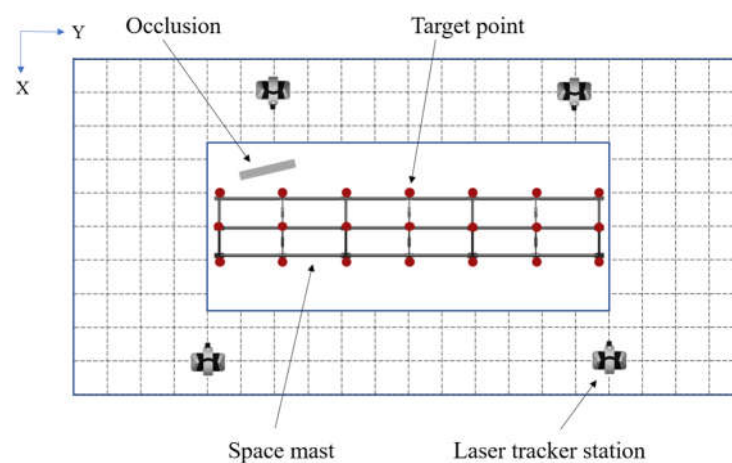

Figure 6. Simulated layout measurement field.

The distance measurement uncertainty of the laser tracker is mainly caused by linear measurement error, ambient temperature variation, and repeated measurements, and is set to $u_{d_j} \approx 3.686 \times 10^{-7} \times l$, where l is the measurement length in meters. As for the station coordinate uncertainty, it is mainly determined by the self-calibration accuracy, and the uncertainty of each coordinate value is set to $u_{X_j} = u_{Y_j} = u_{Z_j} \approx 2\mu m$. The measurement uncertainty of the selected points can then be calculated by the above uncertainty using the GUM method.

The four laser trackers are evenly distributed in space and used as the layout before optimization. Afterwards, the improved CGA is used to solve the spatial optimization layout. The size of the population is set to 50, the number of iterations is 50, and the initial crossover and mutation factors are 0.8 and 0.05. For the existing occlusion, an 18-DOPS bounding box is used to simplify the model, and the normal vectors of the corresponding plane pairs are $(1,0,0)$, $(0,1,0)$, $(0,0,1)$, $(0,1,1)$, $(0,1,-1)$, $(1,0,1)$, $(1,0,-1)$, $(1,1,0)$, $(-1,1,0)$. Finally, the optimal layout position of the laser trackers under the constraints is obtained, and the layout positions of the laser trackers before and after optimization are shown in Figure 7. The spatial coordinate values of the laser trackers before and after the layout optimization are shown in Table 1.
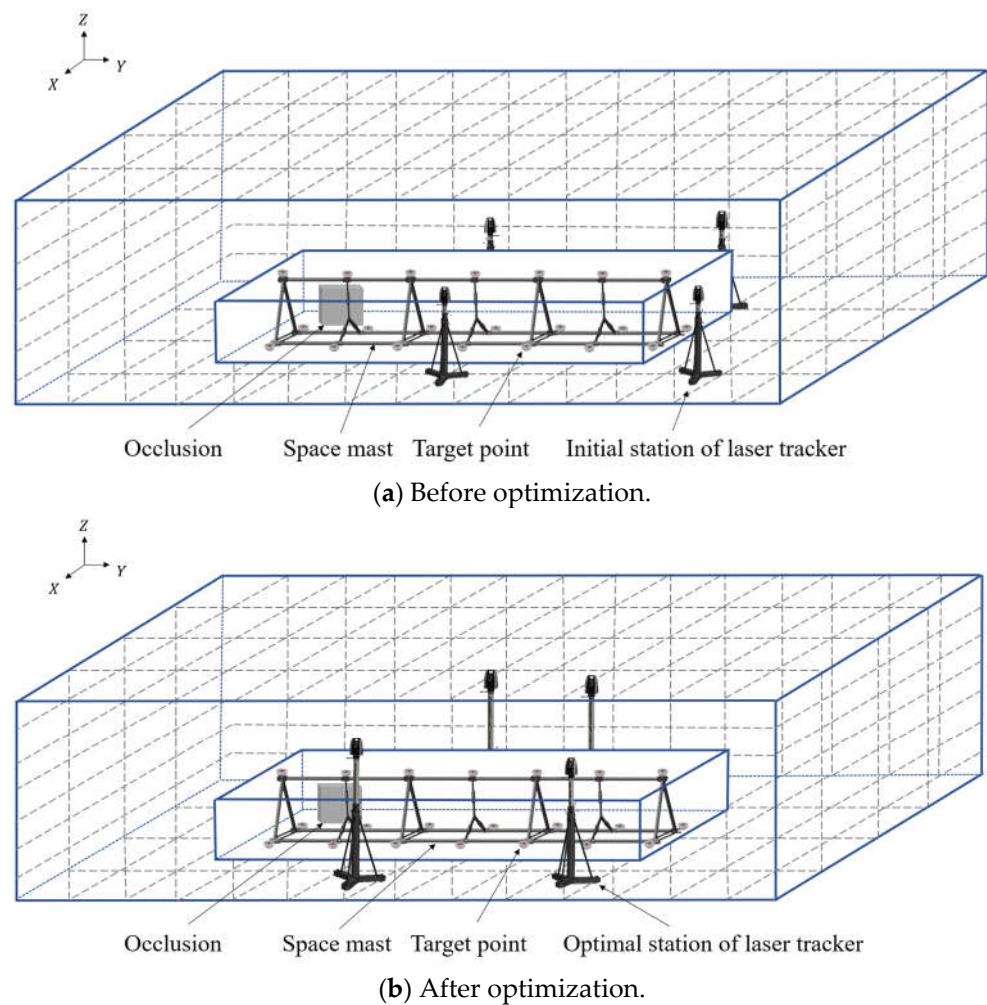
(**a**) Before optimization.

(**b**) After optimization.

Figure 7. The layout of laser trackers for large-scale measurement.

Table 1. Layout of laser trackers before and after the layout optimization.

Laser Tracker Station	Layout/m	
	Before Optimization	**After Optimization**
Laser tracker 1	(2,16,3)	(1.81,13.46,3.90)
Laser tracker 2	(8,16,2)	(8.43,13.86,4.84)
Laser tracker 3	(2,10,3)	(1.81,7.24,4.91)
Laser tracker 4	(8,10,1)	(8.50,10.87,4.91)

Before optimization, there are 11 points that do not meet the constraints. After optimization, all the measurement points can meet the constraints. Ten measurement points that meet the constraints before and after optimization are selected to compare the measurement uncertainty before and after optimization, as shown in Figure 8. The overall average uncertainty of the target points decreases from $43.41\ \mu m$ to $13.40\ \mu m$ after applying the improved CGA. The measurement uncertainty of most points has been significantly reduced, indicating that the optimized layout method can effectively improve measurement accuracy and is suitable for large-scale measurement scenarios with constraints.
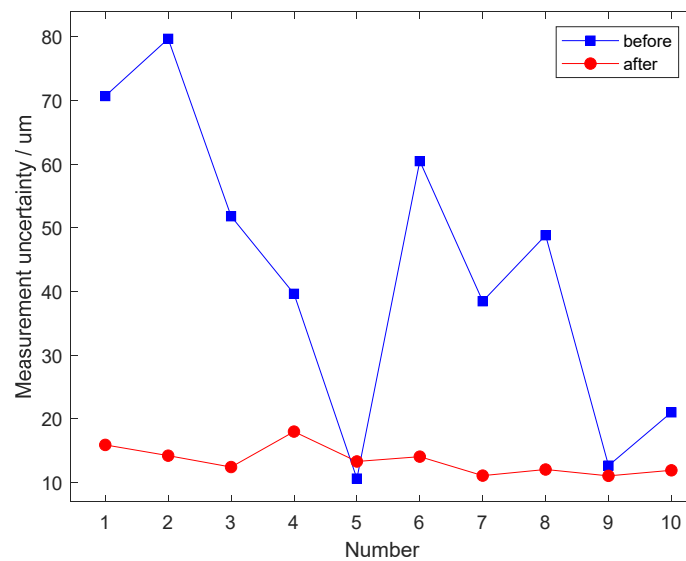
Figure 8. Uncertainty of the selected measurement point before and after optimization.

In order to compare the performance of the improved CGA and traditional GA, the same initial conditions and parameters are used to calculate the normalized convergence results, as shown in Figure 9. Compared with GA, the improved CGA has faster convergence speed and lower fitness. Moreover, the result indicates that the average uncertainty of the measurement points obtained by the improved CGA is lower than that of GA, indicating that the improved CGA algorithm has better global optimization ability and can obtain a better layout position of laser trackers.
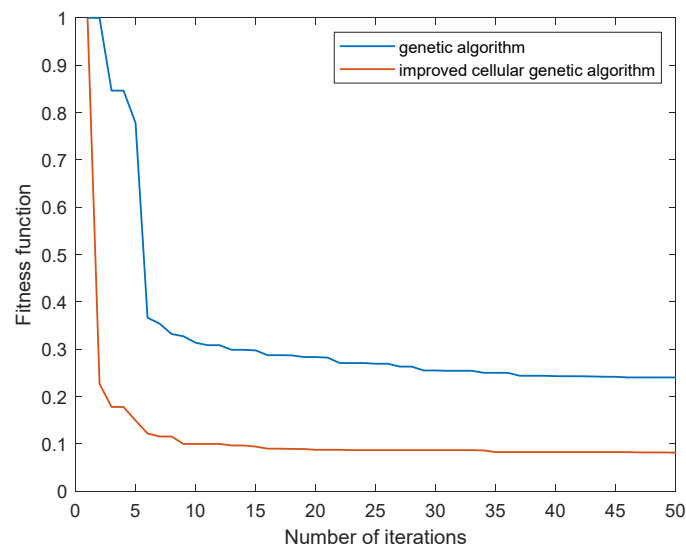

Figure 9. Comparison of fitness between the improved CGA and GA.

6. Conclusions

In this paper, an improved cellular genetic algorithm is proposed to optimize the layout of laser tracker stations in a large-scale multilateral measurement scene. Firstly, the occlusion is simplified by using the k-DOPS bounding box to realize fast intersection detection between the laser beam and the occlusion. Secondly, an adaptive algorithm for adjusting the incident angle of the target ball is proposed to satisfy the constraints of the simultaneous incidence of multiple laser beams. Finally, an improved cellular genetic

algorithm is used to optimize the layout of multiple laser tracker stations. The results show that the optimized layout can ensure the full coverage of the measurement points and reduce the overall measurement uncertainty, showing the feasibility and effectiveness of the proposed method. Compared with the traditional genetic algorithm, the improved cellular genetic algorithm improves the optimization accuracy and convergence speed and can provide an effective laser tracker station layout.

Institutional Review Board Statement: Not applicable.

Informed Consent Statement: Not applicable.

Data Availability Statement: Not applicable.

References

1. Schmitt, R.H.; Peterek, M.; Morse, E.; Knapp, W.; Galetto, M.; Hartig, F.; Goch, G.; Hughes, B.; Forbes, A.; Estler, W.T. Advances in large-scale metrology review and future trends. *CIRP Ann.* **2016**, *65*, 643–665.
2. Guo, H.W.; Deng, Z.Q.; Liu, R.Q. Parameter design and precision measurement of space cable-strut deployable articulated mast. *Opt. Precis. Eng.* **2010**, *18*, 1105–1111.
3. Ran, J.N.; Han, P.T.; Cao, Z.Z.; Wu, J.T.; Zhang, H.J. Overview of Thin-walled Tubular Space Deployable Masts. *Machinery* **2019**, *46*, 44–51.
4. Muralikrishnan, B.; Phillips, S.; Sawyer, D. Laser trackers for large-scale dimensional metrology: A review. *Precis. Eng.* **2016**, *44*, 13–28.
5. Chen, Z.H.; Du, F.Z. Measuring principle and uncertainty analysis of a large volume measurement network based on the combination of iGPS and portable scanner. *Measurement* **2017**, *104*, 263–277.
6. Tang, H.B.; Chao, Y.; Liu, W.H.; Ma, C.X. Review of measurement methods of large-size parts based on machine vision. *Electron. Meas. Technol.* **2021**, *44*, 33–40.
7. Ma, H.Y.; Lin, J.R.; Zhang, R.; Cheng, D.Y.; Zhu, J.G. Research on key technologies for large-scale distributed measurement network reconstruction. *Acta Opt. Sin.* **2021**, *41*, 99–108.
8. Wu, B.; Xu, Y.; Yang, F.T.; Qian, C.Q.; Cai, P. 3D coordinate measuring system based on laser tracking absolute length measurement multilateral method. *Infrared Laser Eng.* **2018**, *47*, 130–135.
9. Takatsuji, T.; Koseki, T.; Goto, M.; Kursawa, T. Restriction on the arrangement of laser trackers in laser trilateration. *Meas. Sci. Technol.* **1998**, *9*, 1357–1359.
10. Takatsuji, T.; Goto, M.; Kirita, A.; Kurosawa, T.; Tanimura, Y. The relationship between the measurement error and the arrangement of laser trackers in laser trilateration. *Meas. Sci. Technol.* **2000**, *11*, 477–483.
11. Wang, Z.; Forbes, A.; Maropoulos, P.G. Laser tracker position optimization. In Proceedings of the 8th International Conference on Digital Enterprise, Stuttgart, Germany, 25–28 March 2014.
12. Aguado, S.; Santolaria, J.; Samper, D.; Aguilar, J.J. Influence of measurement noise and laser arrangement on measurement uncertainty of laser tracker multilateration in machine tool volumetric verification. *Precis. Eng.* **2013**, *37*, 929–943.
13. Hu, J.Z.; Yu, X.F.; Peng, P.; Huang, K.H. Optimal layout of three-dimensional coordinate measurement system based on laser multi-lateration. *Chin. J. Lasers* **2014**, *41*, 108006.
14. Zhang, Y.Y.; Wang, Y.K.; Cui, F.; Xu, K.; Song, X.C. On-site measurement method for large thin-wall tank's ring seam welding based on laser tracker. *Mach. Des. Res.* **2019**, *35*, 144–150.
15. Ren, Y.; Liu, F.F.; Fu, Y.X.; Han. Y.; Zhu, J.G. Placement optimization of laser multilateration network. *Laser Optoelectron. Prog.* **2019**, *56*, 011201.
16. Wang, J.D.; Sun, R.K.; Zeng, X.T.; Wang, Q.J. Research on base station layout of multi-station and time-sharing measurement by laser tracker. *Chin. J. Lasers* **2018**, *45*, 0404005.
17. Aguado, S.; Santolaria, J.; Samper, D.; Aguilar, J.J. Forecasting method in multilateration accuracy based on laser tracker measurement. *Meas. Sci. Technol.* **2017**, *28*, 025011.
18. Tarrio, P.; Bernardos, M.A.; Casar, R.J. Weighted Least Squares Techniques for Improved Received Signal Strength Based Localization. *Sensors* **2011**, *11*, 8569–8592.

19. Choi, J.; Hwang, E.; So, H.Y.; Kim, B. An uncertainty evaluation for multiple measurements by GUM. *Accredit. Qual. Assur.* **2003**, *8*, 13–15.

20. Dorronsoro, B.; Bouvry, P. Cellular genetic algorithms without additional parameters. *J. Supercomput.* **2013**, *63*, 816–835.